Electronic Supplementary Material (ESI) for Journal of Materials Chemistry A.

Supplementary Information for

Unraveling Ni-based layered double hydroxides as high-efficiency electrocatalysts for oxygen evolution reaction: A DFT study

Zhe Xue†, Xinyu Zhang*,†, Jiaqian Qin ‡, and Riping Liu†

†State Key Laboratory of Metastable Materials Science and Technology, Yanshan University, Qinhuangdao 066004, P. R. China

‡Metallurgy and Materials Science Research Institute, Chulalongkorn University, Bangkok 10330, Thailand

***Corresponding Author.**

E-mail: xyzhang@ysu.edu.cn (X. Zhang)

Computational details The binding energies of all reaction intermediates OH*, O*, OOH* were calculated as follows:

$$\Delta E_{OH*} = E(OH*) - E(*) - \left(E_{H2O} - 1/2E_{H2}\right) \quad \text{(S1)}$$

$$\Delta E_{O*} = E(O*) - E(*) - \left(E_{H2O} - E_{H2}\right) \quad \text{(S2)}$$

$$\Delta E_{OOH*} = E(OOH*) - E(*) - \left(2E_{H2O} - {}^{3}/2E_{H2}\right) \quad \text{(S3)}$$

where E(*), E(OH*), E(O*) and E(OOH*) are the DFT total energies of a clean catalyst surface, and that adsorbed by OH*, O* and OOH* species, respectively. E(H_2O) and E(H_2) are the calculated DFT energies of H_2O and H_2 molecule in the gas phase.

Table S1: ZPE and entropic corrections used in this work from Ref.[1]

Species	ZPE	TS
H_2O	0.56	0.67
H_2	0.27	0.41
O*	0.084	0.05
OH*	0.386	0.07
OOH*	0.457	0.16

Table S2: Reaction free energies ΔG_i of intermediate steps (U = 0V) and predicated overpotentials at oxygen active sites.

Samples	$\Delta G_1(eV)$	$\Delta G_2(eV)$	$\Delta G_3(eV)$	$\Delta G_4(eV)$	η(V)
O@Slab	0.94	0.75	**1.88**	1.34	0.65
O@NiCo-o	1.55	0.92	**1.90**	0.55	0.67
O@NiCo-a	**2.15**	0.86	1.30	0.61	0.92
O@NiCo-b	1.41	1.12	**1.97**	0.41	0.74
O@NiCo-c	1.45	0.83	**2.00**	0.64	0.77
O@NiCu-o	**2.98**	0.95	1.82	-0.83	1.75
O@NiCu-a	**2.82**	0.70	1.95	-0.54	1.59
O@NiCu-b	**2.33**	0.31	1.65	0.63	1.10
O@NiCu-c	**2.34**	0.30	1.62	0.66	1.11
O@NiFe-o	**1.59**	1.14	1.52	0.67	0.36
O@NiFe-a	1.61	1.09	**1.98**	0.24	0.75
O@NiFe-b	**1.90**	0.44	1.71	0.87	0.67
O@NiFe-c	**2.33**	0.53	1.51	0.55	1.10
O@NiMn-o	2.50	0.23	**2.52**	-0.33	1.29
O@NiMn-a	1.61	1.49	**1.87**	-0.05	0.64
O@NiMn-b	**1.84**	0.63	1.82	0.64	0.61
O@NiMn-c	**1.85**	0.57	1.27	1.23	0.62
O@NiMo-o	1.01	**1.73**	1.66	0.53	0.50
O@NiMo-a	1.07	1.07	0.61	**2.17**	0.94
O@NiMo-b	1.05	1.33	**1.53**	1.00	0.30
O@NiMo-c	0.88	1.38	0.80	**1.86**	0.63
O@NiW-o	**2.11**	1.21	-0.45	2.05	0.88
O@NiW-a	1.43	1.05	0.45	**1.98**	0.75
O@NiW-b	**1.50**	1.39	1.47	0.56	0.27
O@NiW-c	**1.64**	1.37	0.66	1.25	0.41

The most endoergic step for each reaction site is highlighted in red bold font.

Table S3: Reaction free energies ΔGi of intermediate steps (U = 0V) and predicated overpotentials at metal active sites.

Samples	$\Delta G_1(eV)$	$\Delta G_2(eV)$	$\Delta G_3(eV)$	$\Delta G_4(eV)$	η(V)
Ni@Slab	-0.50	1.54	1.24	**2.63**	1.40
Co@NiCo-0	-0.07	1.28	1.74	**1.96**	0.73
Ni@NiCo-1	1.32	0.78	0.73	**2.09**	0.86
Ni@NiCo-2	**1.38**	1.27	1.37	0.90	0.15
Ni@NiCo-3	0.98	**1.73**	0.95	1.25	0.50
Cu@NiCu-0	1.76	**2.27**	1.54	-0.66	1.04
Ni@NiCu-1	1.44	**1.66**	1.08	0.73	0.43
Ni@NiCu-2	1.39	**1.45**	1.42	0.65	0.22
Ni@NiCu-3	1.24	1.53	**2.15**	-0.01	0.92
Fe@NiFe-0	0.54	0.38	1.99	**2.01**	0.78
Ni@NiFe-1	0.92	0.63	0.74	**2.64**	1.41
Ni@NiFe-2	1.30	**1.44**	1.31	0.87	0.21
Ni@NiFe-3	0.89	0.74	**2.03**	1.26	0.80
Mn@NiMn-0	0.17	0.65	**2.36**	1.73	1.13
Ni@NiMn-1	0.10	1.66	0.96	**2.19**	0.96
Ni@NiMn-2	0.78	1.79	0.54	**1.81**	0.58
Ni@NiMn-3	1.03	**1.47**	1.12	1.29	0.24
Mo@NiMo-0	-0.74	0.28	2.55	**2.82**	1.59
Ni@NiMo-1	-0.29	1.54	1.33	**2.34**	1.11
Ni@NiMo-2	0.09	1.88	0.79	**2.17**	0.94
Ni@NiMo-3	0.60	**1.70**	1.13	1.48	0.47
W@NiW-0	-1.01	0.70	**2.69**	2.54	1.46
Ni@NiW-1	0.02	1.59	1.27	**2.04**	0.81
Ni@NiW-2	0.64	1.36	1.09	**1.83**	0.60
Ni@NiW-3	0.89	**1.85**	0.98	1.19	0.62

The most endoergic step for each reaction site is highlighted in red bold font.

Table S4. The relevant parameters of bond lengths (Å) and charge transitions (e) for different adsorbed intermediates at the optimized reaction sites. The sign of "+" or "-" represents gain or loss electrons, respectively.

Sample		d_{M-O}	d_{O-O}	d_{O-H}	Charge M	$Charge_{O1}$	$Charge_{O2}$	$Charge_H$
O@Slab	O*	1.284			+0.296	+0.102		
	OH*	1.430		0.989	+0.447	+0.503		-0.608
	OOH*	1.447	1.414	1.025	+0.494	-0.010	+0.508	-0.629
Ni@NiFe-2	O*	1.654			- 1.301	+0.446		
	OH*	1.794		0.979	-1.309	+0.951		-0.593
	OOH*	1.838	1.385	1.001	-1.239	+0.312	+0.455	-0.614

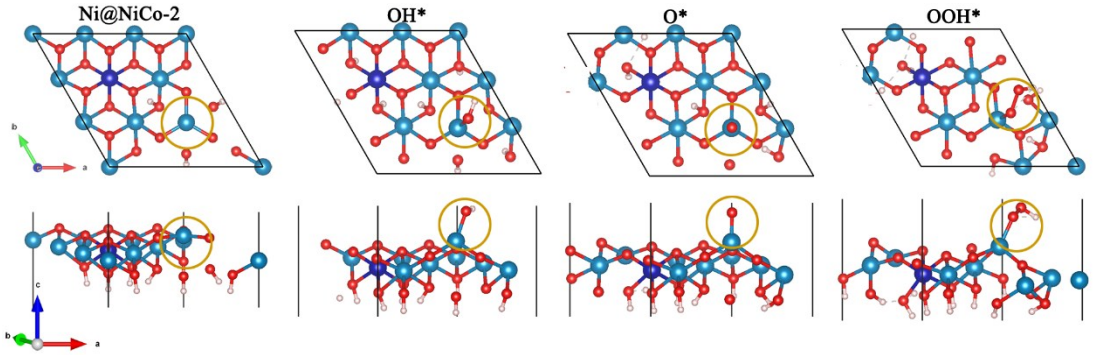

Fig. S1 Top and side views of the optimized intermediates for the Ni@NiCo-2 sample.

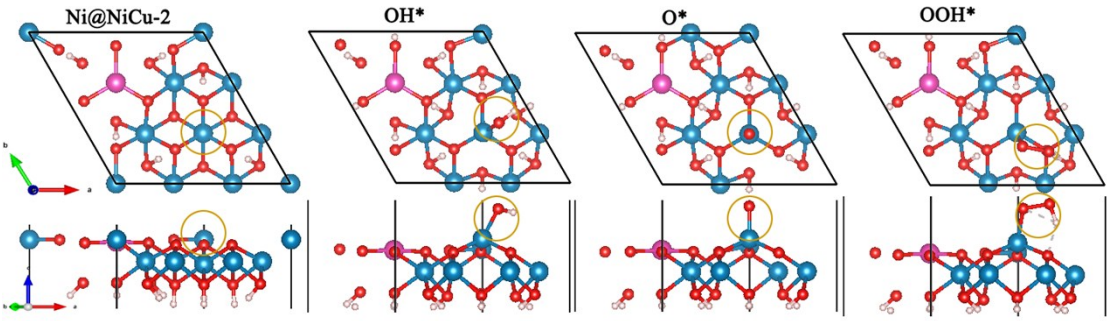

Fig. S2 Top and side views of the optimized intermediates for the Ni@NiCu-2 sample.

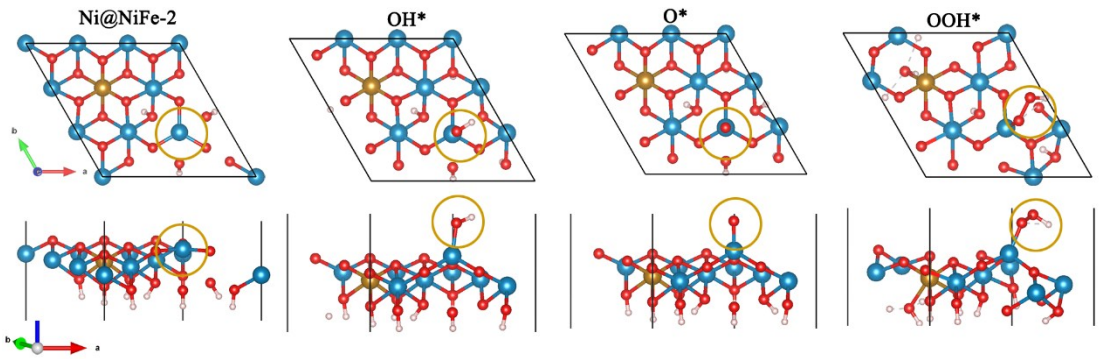

Fig. S3 Top and side views of the optimized intermediates for the Ni@NiFe-2 sample.

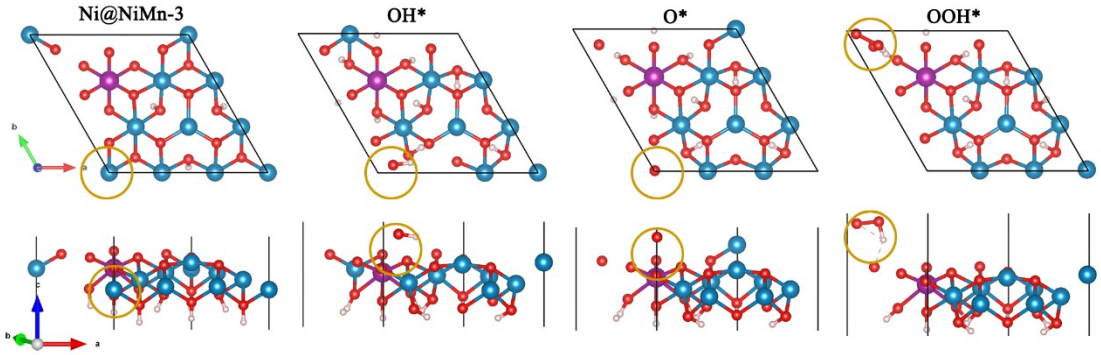

Fig. S4 Top and side views of the optimized intermediates for the Ni@NiMn-3 sample.

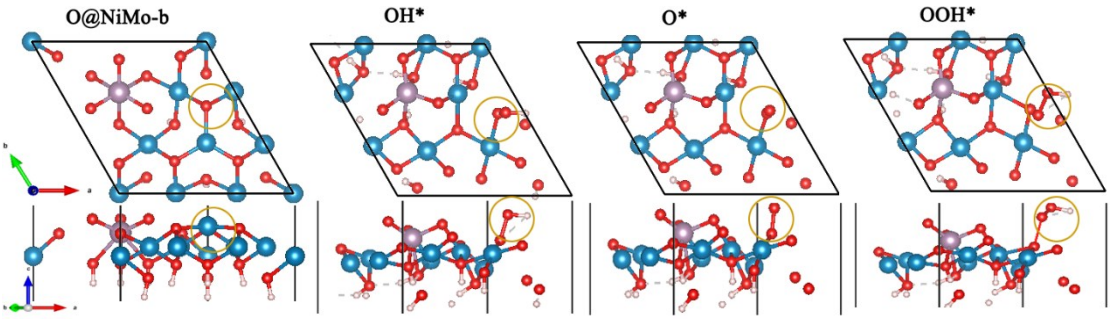

Fig. S5 Top and side views of the optimized intermediates for the O@NiMo-b sample.

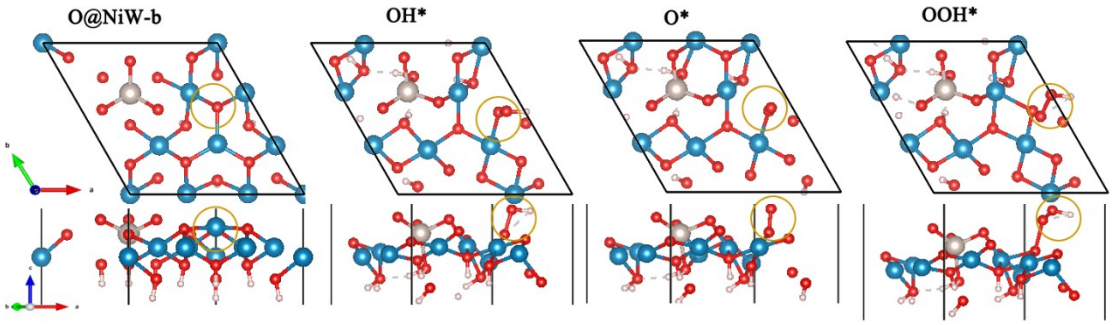

Fig. S6 Top and side views of the optimized intermediates for the O@NiW-b sample.

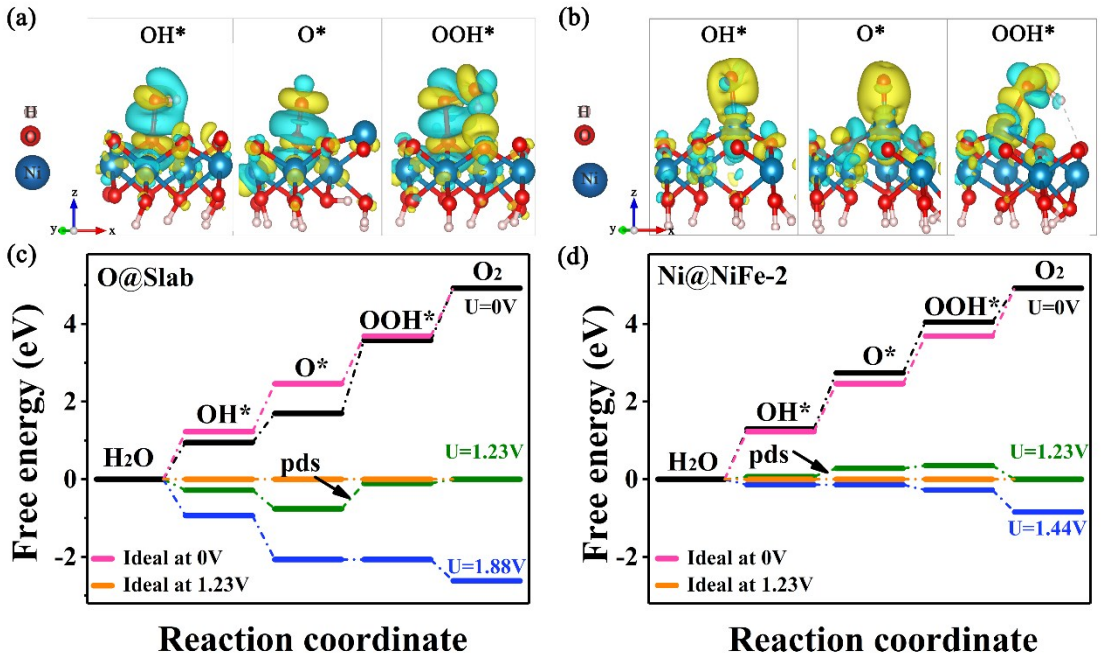

Fig. S7 The optimized structures for OH*, O* and OOH* intermediates as well as the corresponding charge density differences of (a) O@Slab and (b) Ni@NiFe-2 active sites. The electron accumulation and depletion are marked by the yellow and cyan isosurface (0.003 e $Å^{-3}$), respectively. The free energy diagrams of the OER pathway for (c) O@Slab and (d) Ni@NiFe-2 at different applied voltages. The black arrows denote the potential determining step.

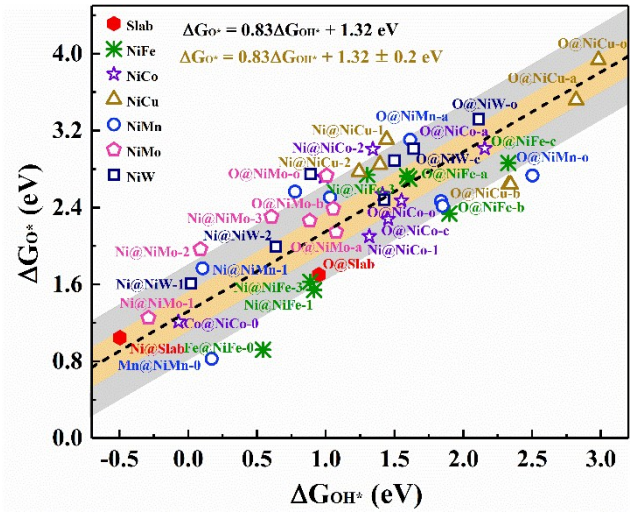

Fig. S8 The scaling relationship between the ΔG_{OH*} and ΔG_{O*} for different reaction sites. Black dashed line represents the line at fit among all considered reaction sites. The yellow and gray region mark ± 0.2, and ± 0.5 eV deviations, respectively.

Reference

1. Li, M.; Zhang, L.; Xu, Q.; Niu, J.; Xia, Z. *J. Catal.,* 2014, **314**, 66-72.